Multiple Cationic Residues of Anthopleurin B That Determine High Affinity and Channel Isoform Discrimination†

Paramjit K. Khera,‡ G. Richard Benzinger,§ Gregory Lipkind,|| Chester L. Drum,§ Dorothy A. Hanck,§ and Kenneth M. Blumenthal*,‡

Department of Molecular Genetics, Biochemistry, and Microbiology, University of Cincinnati College of Medicine, Cincinnati, Ohio 45267-0524, and Departments of Medicine, Pharmacological and Physiological Sciences, and Biochemistry and Molecular Biology, University of Chicago, Chicago, Illinois 60637

Received February 24, 1995; Revised Manuscript Received May 8, 1995⊗

ABSTRACT: Site 3 sea anemone toxins modify inactivation of mammalian voltage-gated Na channels. One variant, anthopleurin A (ApA), effectively selects for cardiac over neuronal mammalian isoforms while another, anthopleurin B (ApB), which differs in 7 of 49 amino acids, modifies both cardiac and neuronal channels with high and approximately equal affinity. Previous investigations have suggested an important role for cationic residues in determination of toxin activity, and our single-site mutagenesis studies have indicated that isoform discrimination can be partially explained by the unique cationic residues Arg-12 and Lys-49 of anthopleurin B (ApB). Here, we have further investigated the role of cationic residues by characterizing toxin mutants in which two such residues are replaced simultaneously. The ApB double mutants R14Q-K48A (cationic residues identical in both ApA and ApB), R12S-K49Q (cationic residues unique to ApB), and R12S-R14Q (cationic residues located in the unstructured loop shared among anemone toxins) were constructed by site-directed mutagenesis and their biological activities characterized by sodium uptake assays in cell lines expressing the neuronal (N1E-115) or cardiac (RT4-B) isoform of the Na channel. Each double mutant displayed reduced activity compared with wild type, but none were completely inactive. Neutralization of the proximal cationic residues (R12 and R14) was the most effective, reducing affinity 72-fold (neuronal) and 56-fold (cardiac). Substitution of cationic residues that differed between ApB and ApA (R12S-K49Q) reduced affinity of the toxin for neuronal channels to a much greater extent than for cardiac channels, producing affinities only slightly lower than for ApA in each case. A structural model for ApB that takes available data into account is proposed. Electrophysiological comparison of ApA, ApB, and the R12S-K49Q mutant confirmed that these two residues are key to the isoform discriminatory ability of ApA. Surprisingly, toxin affinities estimated under voltage clamp, measured in the absence of veratridine and thus most closely reflecting affinity for the closed state of the channels, were greater than estimated by flux for all three toxin forms tested. Of particular note was ApB, which exhibits a 100-fold higher affinity for cardiac channels than estimated previously by flux. We conclude that (1) the residues at positions 12 and 49 are critical for both high affinity and isoform discrimination, (2) of the two arginines, Arg-12 is primarily responsible for maintaining the high binding affinity of ApB to neuronal Na channels, and (3) the cationic nature of Arg-14 is not essential since it can be at least partially compensated for by Arg-12 or one of the two C-terminal lysines. In addition, our data suggest that ApB may also discriminate between closed and open forms of the cardiac Na channel.

Cardiotonic polypeptides found in the venom of the sea anemone *Anthopleura xanthogrammica* bind to voltage-dependent sodium channels of nerve and muscle, maintaining them in an open conformation by delaying their inactivation (Catterall, 1984). One variant, anthopleurin A (ApA), effectively selects for cardiac over neuronal mammalian isoforms while another, anthopleurin B (ApB),[1] which differs in 7 of 49 amino acids and which has been heterologously expressed in this laboratory (Gallagher & Blumenthal, 1992), modifies both cardiac and neuronal channels with high and approximately equal affinity (Gallagher & Blumenthal, 1994). Because anthopleurin toxins are known to have a positive inotropic effect on mammalian heart in whole animals as well as in isolated cardiac preparations, and because neither causes arrhythmias nor affects blood pressure or heart rate (Shibata et al., 1976; Scriabine et al., 1979; Gross et al., 1985; Platou et al., 1986), knowledge of the molecular details of the determinants that control differences in efficacy for these closely related toxins can potentially help in the design of improved cardiotonic drugs that target cardiac Na channels with high specificity.

Chemical modification studies carried out on sea anemone toxins (Newcomb et al., 1980; Barhanin et al., 1981;

† These studies were aided by National Institutes of Health Grants HL-41543 (K.M.B.) and HL-PO1-20592 (D.A.H.). D.A.H. is an Established Investigator of the American Heart Association.

* To whom correspondence should be addressed at the University of Cincinnati College of Medicine (email: BLUMENKM@uc.edu).

‡ Department of Molecular Genetics, Biochemistry, and Microbiology, University of Cincinnati College of Medicine.

§ Departments of Medicine and Pharmacological and Physiological Sciences, University of Chicago.

|| Department of Biochemistry and Molecular Biology, University of Chicago.

⊗ Abstract published in *Advance ACS Abstracts,* June 15, 1995.

[1] Abbreviations: ApA(B), anthopleurin A(B) (neurotoxins A and B from *Anthopleura xanthogrammica*); AsI, neurotoxin I from *Anemonia sulcata*; ShI, neurotoxin I from *Stichodactyla helianthus*.

0006-2960/95/0434-8533$09.00/0

Chart 1

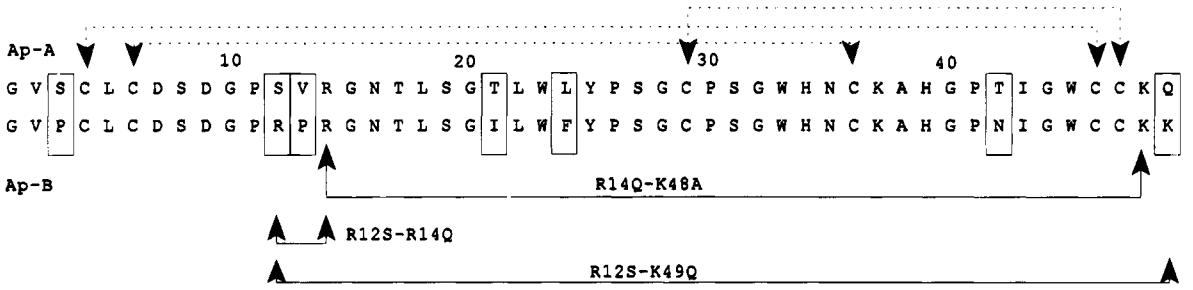

Kolkenbrock et al., 1983; Mahnir et al., 1989; Gould et al., 1990) and functionally similar α-scorpion toxins (El Ayeb et al., 1986; Kharrat et al., 1989) in different laboratories have indicated the importance of cationic residues as determinants of toxin activity. We previously reported the generation of a panel of mutants at the two unique cationic sites of ApB, Arg-12 and Lys-49, which are replaced by neutral residues having hydrogen bond forming capabilities in ApA, and at Arg-14 and Lys-48, which are the two cationic residues conserved among all known sea anemone toxins. Characterization of the effects of these mutant toxins upon sodium uptake into excitable cells revealed that replacement of Arg-14, Lys-48, or Lys-49 had relatively minor effects on the activity of ApB (Gallagher & Blumenthal, 1994; Khera & Blumenthal, 1994), whereas mutation of Arg-12 reduced the apparent affinity of the toxin for both the neuronal and cardiac channels (Gallagher & Blumenthal, 1994).

We therefore postulated that pairs of cationic residues might control toxin preference for the cardiac isoform of the sodium channel. Utilizing the techniques employed for the synthesis of fully active ApB (Gallagher & Blumenthal, 1992), we constructed a series of doubly mutated forms of this toxin as shown in Chart 1. Disulfide bonds are indicated with dashed lines and residues that differ between toxins by boxes. Functional characterization of these mutants (indicated by solid lines), R14Q-K48A (charged residues identical in both ApA and ApB), R12S-K49Q (charged residues unique to ApB), and R12S-R14Q (cationic sites within the unstructured Arg-14 loop), has been accomplished by measuring their ability to synergistically enhance veratridine-dependent $^{22}Na^+$ uptake in cell lines that express the neuronal (N1E-115 murine neuroblastoma cells) or cardiac (rat cell line RT4-B) isoforms of the sodium channel. In addition, the R12S-K49Q double mutant was evaluated electrophysiologically in comparison with the parents ApA and ApB. Each double mutant displayed reduced activity compared with wild type, but none were completely inactive. In ion flux studies, neutralization of the adjacent cationic residues (R12 and R14) was the most effective, reducing affinity 72-fold (neuronal) and 56-fold (cardiac). Substitution of cationic residues that differed between ApB and ApA (R12S-R49Q) reduced affinity of the toxin for neuronal channels to a much greater extent than for cardiac channels, yielding $K_{0.5}$ values only slightly lower than for ApA. Thus, analysis of toxin-dependent ion fluxes demonstrates that the cationic residues Arg-12 and Lys-49 are responsible for virtually all of the functional differences between these two cardiotonic polypeptides. Electrophysiological characterization of ApA, ApB, and the R12S-K49Q mutant is also consistent with this conclusion and furthermore suggests that all three toxins bind with greater affinity to the closed conformation of the Na channel. This apparent state dependence of toxin binding is particularly pronounced for the interaction of ApB and the R12S-K49Q mutant with cardiac channels, wherein binding to the closed state is favored by 50−100-fold.

EXPERIMENTAL PROCEDURES

Cell Cultures. The rat peripheral neurotumor cell line RT4-B, known to express predominantly the cardiac/denervated skeletal muscle sodium channel (Donahue et al., 1991; Zeng et al., 1993), was generously made available by Dr. Laurie Donahue (Health Sciences Center, Texas Tech University), and the murine neuroblastoma cell line N1E-115 was kindly provided by Dr. Marshall Nirenberg (National Heart, Lung, and Blood Institute, NIH). All cells were propagated in high glucose Dulbecco's modified Eagle's medium containing 10% fetal calf serum supplemented with 110 units per milliliter each of penicillin and streptomycin in a humid atmosphere containing 10% CO_2. Cells were grown to confluency in 24 well plates for sodium uptake experiments. N1E-115 cells were then subsequently maintained for an additional 48 h in differentiation medium containing 1.5% each of fetal calf serum and dimethyl sulfoxide prior to use in sodium flux assays. While the effect of this treatment on the expression of functional sodium channels is not well documented, we have consistently noted that it serves to enhance the adherence of N1E-115 cells to plasticware, thus facilitating their use in ion flux assays.

Mutant Constructions. Three double mutants of ApB were constructed to target four of the five cationic residues of this toxin. The mutant R14Q-K48A represents the simultaneous mutation of the two conserved cationic sites of anemone toxins, while the R12S-K49Q mutant probes the two cationic residues unique to ApB. The R12S-R14Q mutant includes both the cationic sites of the Arg-14 loop which is common to anemone toxins (Norton, 1991). All double mutants were constructed by site-directed mutagenesis using the polymerase chain reaction. The expression vector pKB13,[2] in which the ApB gene is fused to the 3′ end of gene 9 of bacteriophage T7, was used as a template. Each of 30 PCR cycles consists of melting at 94 °C for 1 min, annealing for 2 min at 42 °C, and polymerizing at 72 °C for 2 min. The mutant R14Q-K48A was generated by mutating the Arg-14 site (bold) with the sense strand primer 5′-TTCTGAT*GGGC-CC*AGACCC**CA**AGGTAAC-3′, which includes the *Apa*I restriction site of the ApB gene (italics), and the antisense primer 5′-CGGGC*GAGCTC*TTATTACTT**CG**CACAGC-3′, which includes the Sst1 restriction site and simultaneously

[2] B. L. Dias-Kadambi and K. M. Blumenthal, unpublished studies.

mutates the Lys-48 (bold) codon. The Arg-12 and Arg-14 sites of the R12S-R14Q double mutant were targeted using the sense primer 5′-TTCTGAT*GGGCCC***AG**CCCC**AA**G-GTAAC-3′ and the wild-type antisense primer 5′-GTTCG-GA*CCATGG*GCTTT-3′, which includes the *Nco*I restriction site of the ApB gene. To obtain the R12S-K49Q mutant, the Arg-12 and Lys-49 residues were mutated using the sense primer 5′-TTCTGAT*GGGCCC***AG**CCCCAGAGG-3′ in combination with the antisense primer 5′-CGGGC*GAGCTC*T-TATTA**CTG**CTTACAG-3′. The *Apa*I/*Sst*I or *Apa*I/*Nco*I fragments of the PCR products were inserted into the plasmid pKB13 following digestion by the appropriate restriction enzymes. Sequences of all the mutants were confirmed prior to protein expression by double-stranded dideoxy chain termination (Sanger et al., 1980).

Expression and Purification of Mutant ApB Proteins. The expression and purification procedure has been described in detail previously (Gallagher & Blumenthal, 1992). In brief, the expression vector pKB13 and the *Escherichia coli* strain BL21(DE3) were used to express high levels of mutant and wild-type fusion proteins which were then purified by anion-exchange chromatography on DE52. Following reoxidation of the disulfide bonds using redox couples of glutathione, all fusion proteins were hydrolyzed overnight at 37 °C with staphylococcal protease (0.75% by weight). The cleaved toxins were then purified to homogeneity by reverse-phase HPLC.

Analytical Methods. Prior to amino acid analysis, performic acid oxidation was carried out on 2 nmol of each purified toxin to convert cysteine residues to cysteic acid. The oxidized samples were then hydrolyzed in the presence of constant boiling HCl *in vacuo* at 110 °C for 22 h. Finally, samples were derivatized with phenyl isothiocyanate and analyzed by HPLC on a Pico Tag column.

To estimate protein secondary structures, far-UV circular dichroism spectra of wild-type and mutant toxins were measured using a Jasco J-710 spectropolarimeter with samples dissolved in 5 mM sodium phosphate buffer, pH 6.8. Thermal denaturation studies were carried out in the presence of 1.5 M guanidine hydrochloride in a water-jacketed quartz cell. Quantitative estimates of secondary structures were derived by comparison of the spectral data to a least-squares fit of a composite structure based on the known structures of myoglobin, egg white lysozyme, ribonuclease A, papain, cytochrome *c*, hemoglobin, α-chymotrypsin, trypsin, and horse liver alcohol dehydrogenase.

Functional Characterization of Recombinant and Mutant ApB Proteins. The ability of ApB to enhance veratridine-dependent $^{22}Na^+$ uptake by cultured cells was utilized to measure the biological activities of wild-type and mutant toxins. N1E-115 cells express the tetrodotoxin-sensitive neuronal, and RT4-B cells the tetrodotoxin-resistant cardiac, isoform of the sodium channel. Cells maintained at 37 °C were pretreated in Na-free medium with 20 μM veratridine and increasing concentrations of wild-type and mutant toxins; the absence of Na^+ during preincubation prevents dissipation of the membrane potential due to channel activation. Initial rates of uptake were then measured over a 1 min time course in the presence of the same concentrations of effectors and 10 mM [^{22}Na]NaCl (Gallagher & Blumenthal, 1992; Schweitz et al., 1981). Uptake rates were corrected for the sodium flux due to 20 μM veratridine alone, and the kinetic constants $K_{0.5}$ and V_{max} were obtained by fitting the experimental data to a hyperbolic function by the method of Cleland (1979). In these assays, a $K_{0.5}$ value for sodium uptake represents the effect of a mutation on apparent toxin affinity for the sodium channel, and a V_{max} value reflects the ability of a toxin to maintain the channel in its open conformation.

Electrophysiological Methods. (a) Preparations and Solutions. Cultured cells were dissociated from substrates mechanically (N1E-115) or through incubation for 2−4 min in 0.25% trypsin with 1 mM EDTA (no. 25200, Gibco BRL, Gaithersburg, MD) (RT4-B). Cells were washed and resuspended in control extracellular solution, which consisted of (in mM) 70 or 35 Na^+, 70 or 105 Cs^+, 2.5 K^+, 1.0 Mg^{2+} 0.5 Ca^{2+}, 145.5 Cl^-, and 10 HEPES (pH 7.4, titrated with CsOH). The Na^+/Cs^+ concentrations were adjusted to provide I_{Na} between 1 and 4 nA. For treatment with toxins, control extracellular solution was supplemented with 1 mg/mL bovine serum albumin (no. A-6003, Sigma, St. Louis, MO) and varying concentrations of toxin. The pipet solution consisted of (in mM) 140 Cs^+, 130 F^-, 10 Cl^-, and 10 HEPES (pH 7.4, titrated with CsOH). Experiments were performed at 24 °C. ApA toxin was obtained from Sigma.

(b) Recording Techniques and Experimental Protocols. Recordings were made in the whole-cell patch configuration. I_{Na} was measured using an Axopatch 200 amplifier (Axon Instruments, Foster City, CA). Voltage protocols, using CLAMPEX 6.0.1 (Axon Instruments) on an 486-50 microcomputer, were imposed from a 12-bit DA converter. Data were filtered at 10 kHz with a four-pole Bessel filter and digitized at 12-bit resolution at 50 kHz. High-resistance seals were allowed to form, using patch pipets with resistances of 1.0−2.0 MΩ, in a chamber containing control extracellular solution. Once whole-cell access was achieved, cells were clamped at a potential of −140 mV (RT4-B) or −110 mV (N1E-115), which ensured complete availability of Na^+ channels. Control of voltage was assayed by examination of the time course of the capacitive current in response to 10 mV changes in membrane potential and by examination of the negative slope region of the peak current−voltage relationship.

Sealed cells were transferred to a chamber containing toxin solution, and modification was monitored with depolarizing pulses, with durations of 10 ms (RT4-B) or 11 ms (N1E-115), to −10 mV (Figure 1). Pulses were evoked at frequencies ranging from $^1/_3$ to 1 Hz, which caused cells to be depolarized for ≤1.1% of the total period of modification. After modification was complete, cells were returned to the control chamber, and washout was monitored with similar depolarizing trains (Figure 1). Pulses during washout were evoked at frequencies ranging from $^1/_{30}$ to $^1/_5$ Hz, which caused cells to be depolarized for ≤0.22% of the total period of washout.

(c) Analysis. Modification and unmodification were assayed by monitoring I_{Na} at a time sufficiently distant from the onset of depolarization for unmodified channels to have reached nearly complete inactivation. Specifically, traces were corrected for ohmic leak, and current was averaged over a 1 ms window centered at 9.5 (RT4-B) or 7.5 (N1E-115) ms. Because the development of modification by anthopleurin toxins was extremely slow at concentrations near $K_{0.5}$, similar to rates predicted from $^{22}Na^+$ flux studies (Gallagher & Blumenthal, 1992), toxin affinities were determined through the identity

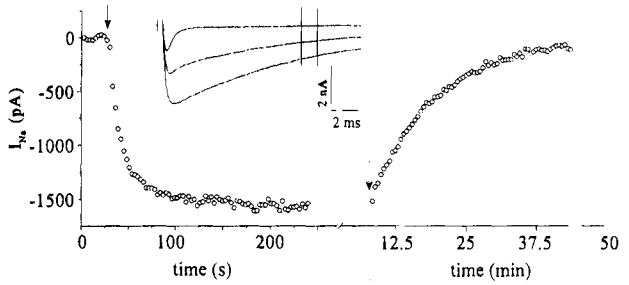

FIGURE 1: Development and washout of toxin-induced delay in inactivation. Shown is example I_{Na} in a RT4-B cell, which was modified to steady state with 40 nM ApB (R12S-K49Q) toxin. The inset shows I_{Na} evoked during depolarizations to −10 mV during washout of toxin at 0 s (lower) and 7.5 s (middle), and 25 min (upper), after the return of the cell to the toxin-free bath. Traces are shown leak-corrected. R_L = 1.1 GΩ; C_M = 49 pF (cell 94824058). The bars denote the 1 ms window of current averaged for analysis of the time courses. The placement of the window was chosen such that unmodified I_{Na} had decayed nearly completely, leaving only toxin-modified channels as carriers of the residual current. The graph shows the time course relative to the beginning of the recording of the increase in current as channel modification proceeded (solid arrow) and the time course of the reversal of the delay in inactivation of I_{Na}, which occurred after transfer of the cell to toxin-free solution (broken arrow). Note the difference in time scale between the two panels. This effect was qualitatively similar across all channel isoforms under study and was produced equivalently by all forms of toxin at suitable concentrations.

$$K_D = k_{off}/k_{on}$$

where k_{on} and k_{off} represent the rate constants for association and dissociation of toxin from the channel. k_{off} was determined from the fit of washout data with a single decaying exponential. Toxin concentration ([T]) was assumed to be 0. k_{on} was determined similarly from the apparent rate of channel modification and the relation:

$$k_{mod} = k_{on}[T] + k_{off}$$

For most combinations of toxin and channel isoforms, a mean value of k_{off} was determined from washout data from multiple cells, and this k_{off} was used to obtain estimates for k_{on} from the time course of channel modification in toxin washin experiments. For modification of cardiac channels by ApB R12S-K49Q, k_{on} was estimated by the slope of the dependence of k_{mod} on toxin concentration. Fitting was performed using CLAMPFIT 6.0.1, and additional analysis utilized ORIGIN 3.5.2 (Microcal Software, Northampton, MA). Values given are means ± standard error.

RESULTS

Reoxidation and Cleavage of Fusion Proteins. The amount of fusion protein obtained in the case of each of the double mutants was comparable to that obtained for wild-type recombinant toxin. After cleavage of the fusion protein with staphylococcal protease, purification by reverse-phase HPLC yielded equivalent amounts of the wild-type and mutant proteins. These results suggest that none of the targeted sites represent essential folding determinants, as anticipated from previous analyses of the single-site mutants (Gallagher & Blumenthal, 1994; Khera & Blumenthal, 1994). The HPLC elution profiles show that all double mutants have slightly longer retention times than wild type, as was observed previously for the R14A, R14Q, K48A, and K48Q mutants (Khera & Blumenthal, 1994), presumably due to the increased hydrophobicity caused by these substitutions.

Table 1: Amino Acid Compositions of Anthopleura Toxins

	residues/mol[a]			
amino acid	ApB	R14Q-K48A	R12S-K49Q	R12S-R14Q
aspartic acid	4.7 (5)	5.0 (5)	5.1 (5)	5.0 (5)
glutamic acid	0.6 (0)	1.6 (1)	1.8 (1)	2.4 (1)
cysteine[b]	4.0 (6)	4.2 (6)	4.2 (6)	3.6 (6)
serine	3.6 (4)	3.7 (4)	4.6 (5)	4.2 (5)
glycine	8.0 (8)	8.4 (8)	8.3 (8)	8.0 (8)
histidine	1.7 (2)	1.9 (2)	2.0 (2)	1.7 (2)
threonine	1.3 (1)	1.1 (1)	1.1 (1)	1.1 (1)
alanine	1.4 (1)	2.2 (2)	1.2 (1)	1.6 (2)
arginine	2.1 (2)	1.0 (1)	1.0 (1)	0.2 (0)
proline	5.9 (6)	5.5 (6)	5.5 (6)	5.3 (6)
tyrosine	0.9 (1)	0.8 (1)	0.7 (1)	0.6 (1)
valine	1.4 (1)	1.1 (1)	1.1 (1)	1.2 (1)
methionine	0.1 (0.)	0.1 (0)	(0)	0.1 (0)
isoleucine	2.3 (2)	1.9 (2)	2.1 (2)	2.0 (2)
leucine	3.2 (3)	2.8 (3)	3.0 (3)	3.0 (3)
phenylalanine	1.3 (1)	0.8 (1)	0.9 (1)	0.9 (1)
lysine	2.9 (3)	1.7 (2)	1.9 (2)	2.5 (3)
tryptophan[c]	(3)	(3)	(3)	(3)

[a] Not corrected for partial degradation of serine and threonine during acid hydrolysis. [b] Determined as cysteic acid after performic acid oxidation. [c] Determined spectrophotometrically.

Structural Characterization of Mutant Proteins. The amino acid compositions of the purified double mutant proteins confirm the substitutions designed in each case (Table 1). The somewhat elevated levels of glutamic acid observed are a system artifact. N-Terminal sequence analysis of toxins produced as described above is consistent with the anticipated primary structures and reveals no evidence for glutamate-containing N-terminal extensions. Far-UV circular dichroism spectra of the three mutant toxins measured over the range 190−250 nm are indistinguishable from those of wild-type ApB. Secondary structure estimations derived from the spectral data indicate that, like wild-type ApB, all three mutant proteins exist primarily in a β-sheet conformation, with contents of 57−62%, and none contain a significant amount of α-helix.

To compare the structural stabilities of the double mutants to that of the wild-type toxin, thermal denaturation experiments were carried out over the temperature range 20−80 °C in the presence of 1.5 M guanidine hydrochloride. The CD spectra recorded under these conditions show that all three toxins retain full secondary structure throughout this temperature range (data not shown), demonstrating that neither the secondary structure nor the stability of ApB is affected even upon simultaneous replacement of any two cationic sites within the cluster.

Functional Characterization by Ion Flux. The ability of wild-type and mutant forms of ApB to enhance veratridine-dependent sodium uptake was measured in cultured cells expressing either the neuronal (N1E-115) or cardiac (RT4-B) isoform of the sodium channel. Dose−response curves for recombinant ApB and the R12S-K49Q double mutant in N1E-115 cells are compared in Figure 2, and those for the cardiac channels are shown in Figure 3. The concentration of wild-type toxin yielding half-maximal uptake of sodium in N1E-115 cells is 22 nM, consistent with previous data from this (Gallagher & Blumenthal, 1994; Khera & Blumenthal, 1994) and other laboratories (Schweitz et al., 1981; Kem et al., 1989). The toxin dependence of uptake in RT4-B

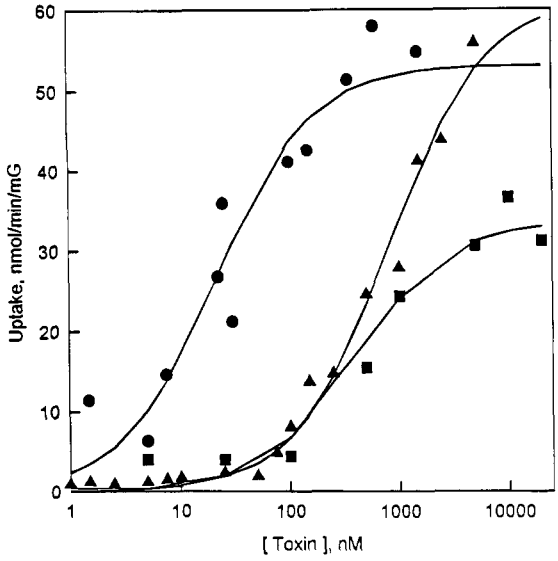

FIGURE 2: Veratridine-dependent sodium uptake by N1E-115 cells. The synergistic effect of wild-type ApB (●), ApA (■), and the ApB mutant R12S-K49Q (▲) on uptake induced by 20 μM veratridine. The uptake rates shown have been corrected for that due to veratridine alone, and all uptakes are abolished in the presence of 100 nM tetrodotoxin.

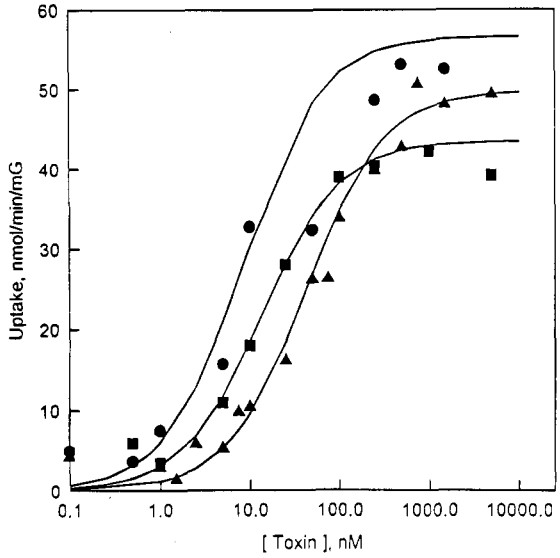

FIGURE 3: Veratridine-dependent sodium uptake by RT4-B cells. The synergistic effect of wild-type ApB (●), ApA (■), and the ApB mutant R12S-K49Q (▲) on uptake induced by 20 μM veratridine. The uptake rates shown have been corrected for that due to veratridine alone.

cells is also in excellent agreement with previous measurments (Gallagher & Blumenthal, 1994).

Figure 4 compares the $K_{0.5}$ for all toxin variants and channels tested. The apparent affinities of all three double mutants for neuronal channels are decreased significantly. The R14Q-K48A, R12S-K49Q, and R12S-R14Q toxins have $K_{0.5}$ values of 592, 818 and 1588 nM, respectively, corresponding to 27-, 37-, and 72-fold lower affinity than wild-type ApB. In comparison to the single-site cationic mutations of ApB characterized previously (Gallagher & Blumenthal, 1994; Khera & Blumenthal, 1994), which reduced affinity only between 1.4- and 18-fold, simultaneous double mutations of these cationic sites synergistically reduce toxin activity. Replacement of both the arginines (R12S-R14Q) with neutral, hydrogen bond donor residues has the

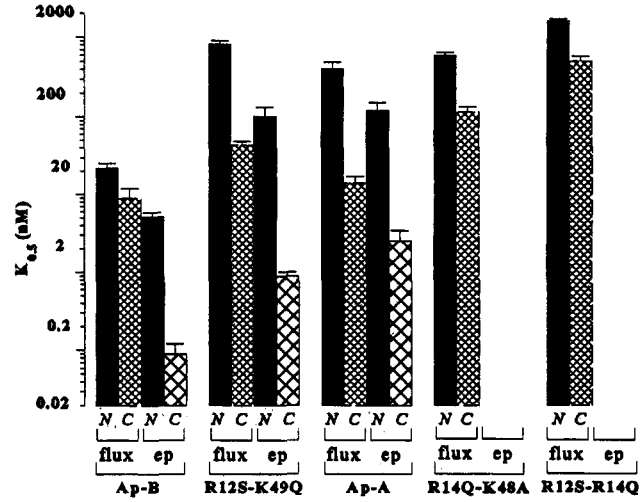

FIGURE 4: Comparison of $K_{0.5}$ determined by veratridine-dependent sodium uptake and K_D determined by electrophysiology for neuronal (N) and cardiac (C) channels. Data are graphed on a log scale ± SE of the estimate. $K_{0.5}$ and K_D used in the graph are those given in Table 2.

most drastic effect on toxin activity for both neuronal and cardiac channels. The $K_{0.5}$ of this toxin for neuronal Na channels was greater than 1 μM, necessitating very high toxin concentrations to attain saturation, and so our estimates of $K_{0.5}$ and V_{max} in the N1E-115 line may be subject to a greater degree of uncertainty than are the remaining data sets. Nonetheless, the R12S-R14Q mutant remains active against both channel isoforms. We interpret these results to mean that the presence of at least one cationic residue within the Arg-14 loop is important for the ability of ApB to bind efficiently to the channel and perhaps to stabilize its open conformation once bound.

In RT4-B cells, which express the cardiac isoform of the sodium channel, all mutations reduced affinity, but the R12S-K49Q combination inactivated least. Moreover, isoform discrimination by this mutant was very similar to that seen when comparing ApA to ApB. Maximum uptake of sodium by all three mutants reaches almost the normal value in these cells. Hence, all mutants are able to stabilize the open conformation of the cardiac sodium channel to roughly the same extent. Kinetic constants derived from the ion flux data for all toxin forms are summarized in Table 2.

Functional Characterization by Electrophysiology. Analysis of R12S-K49Q and of wild-type ApB and ApA by whole-cell voltage clamp both confirms and extends these results. Sodium current (I_{Na}) was monitored during modification and unmodification of channels in both RT4-B and N1E-115 cells, yielding values of k_{on}, k_{off}, and K_D as described in Experimental Procedures. Consistent with the behavior of the wild-type toxins (Warashina &Fujita, 1983; Wasserstrom et al., 1993), R12S-K49Q produced a marked slowing of current decay in response to depolarization: the time courses of I_{Na} fully modified by the various toxin forms were very similar for each isoform of the channel. A comparison of the time constants of decay of I_{Na} at −10 mV after complete modification by each form of the toxin indicated that there were no differences in I_{Na} decay in N1E115 cells [in ms: τ_{ApA}, 4.3 ± 0.3 (n = 4); τ_{ApB}, 4.2 ± 0.3 (n = 5); $\tau_{R12S\text{-}K49Q}$, 4.3 ± 0.1 (n = 3)], and I_{Na} time constants of decay varied less than 2-fold in RT4B cells [in ms: τ_{ApA}, 7.2 ± 0.5 (n = 4); τ_{ApB}, 13 ± 0.6 (n = 3); $\tau_{R12S\text{-}K49Q}$, 10 ± 0.6 (n = 8)].

Table 2: Kinetics of Anthopleura Toxin Action

	Electrophysiology					
	k_{on} (10^6 s^{-1} M^{-1})		k_{off} (10^{-3} s^{-1})		K_D (nM)	
toxin	neuronal	cardiac	neuronal	cardiac	neuronal	cardiac
ApB	0.93 ± 0.11 (n = 3)	1.4 ± 0.40 (n = 3)	4.7 ± 0.12 (n = 3)	0.13 ± 0.01 (n = 3)	5.1 ± 0.7	0.09 ± 0.03
R12S-K49Q	0.27 ± 0.08 (n = 7)	1.1 ± 0.1 (n = 11)	27 ± 3 (n = 6)	1.0 ± 0.1 (n = 6)	100 ± 31	0.89 ± 0.11
ApA	0.35 ± 0.08 (n = 7)	1.4 ± 0.37 (n = 3)	41 ± 1 (n = 3)	3.5 ± 0.64 (n = 3)	120 ± 30	2.5 ± 0.9

	Ion Flux			
	$K_{0.5}$ (M)		V_{max} (nmol min^{-1} g^{-1})	
toxin	neuronal	cardiac	neuronal	cardiac
ApB	22 ± 3	9 ± 3	53 ± 2	57 ± 4
R14Q-K48Q	592 ± 55	115 ± 17	56 ± 2	43 ± 2
R12S-K49Q	818 ± 82	43 ± 3	61 ± 3	50 ± 1
R12S-R14Q	1588 ± 127	504 ± 71	15 ± 1	62 ± 3
ApA	400 ± 83	14 ± 3	33 ± 1	43 ± 2

These data suggest that the large differences in affinity between toxin variants do not arise simply because these peptides produce different rates of entry into a low-affinity inactivated state. As described in Experimental Procedures, we monitored the time course of the development and disappearance of current in washin and washout experiments in order to determine values of k_{on}, k_{off}, and K_D. Grouped data are given in Table 2. Values of K_D were qualitatively similar to those obtained by $^{22}Na^+$ flux, with R12S-K49Q displaying affinities closer to those of ApA than ApB for both cardiac and neuronal channel isoforms (Table 2, Figure 4). However, toxin affinities obtained with this technique were dramatically greater than those obtained in flux studies (Gallagher & Blumenthal, 1994; Khera & Blumenthal, 1994). This discrepancy is particularly large for the binding of wild-type ApB to cardiac channels, for which biochemical and electrophysiological affinities differ by a factor of 100, and to a lesser extent for R12S-K49Q, for which the difference is approximately 50-fold (Figure 4); a potential explanation for this discrepancy is provided in the Discussion.

The relative ordering of toxin affinities was determined primarily by k_{off}. Values of k_{on} differ by less than 10-fold among tested combinations of channel and toxin, while off rates vary from 41 × 10^{-3} (ApA / neuronal) to 0.13 × 10^{-3} s^{-1} (ApB/cardiac), a factor of 320. Figure 5, which depicts the time course of toxin washouts, illustrates this span of values.

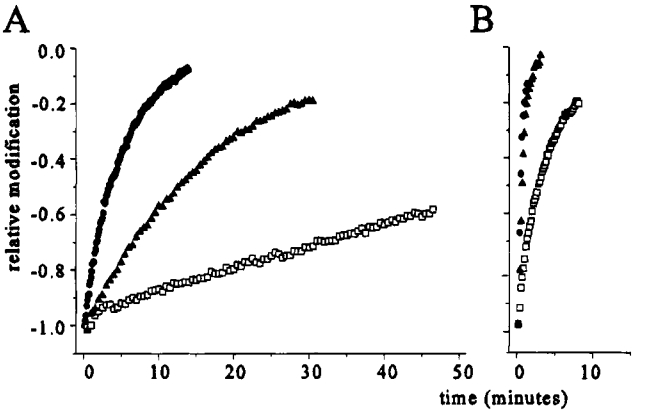

FIGURE 5: Time courses of washout of ApA, ApB, and R12S-K49Q for cardiac (left) and neuronal (right) cells. In each case, a subset of the data in Table 3was normalized using the asymptotes determined from single-exponential fits to the individual data sets and the initial magnitudes of current. Means of these data are graphed as follows. (Left) Cardiac channels in RT4-B cells: (●) ApA, n = 3; (□) ApB, n = 3; (▲) ApB R12S-K49Q, n = 6. (Right) Neuronal channels in N1E-115 cells: (●) ApA, n = 2; (□), ApB, n = 2; (▲) ApB R12S-K49Q, n = 5.

DISCUSSION

In chemical modification studies, cationic residues of sea anemone toxins (Newcomb et al., 1980; Barhanin et al., 1981; Kolkenbrock et al., 1983; Mahnir et al., 1989; Gould et al., 1990) and functionally similar α-scorpion toxins (El Ayeb et al., 1986; Kharrat et al., 1989) have been found to be important for determining toxin activity. When studied by single-site mutation, four out of five cationic residues of recombinant ApB have been shown to contribute to this toxin's binding affinity for the sodium channel (Gallagher & Blumenthal, 1994; Khera & Blumenthal, 1994). However, it should be emphasized that while mutation at one of these sites, Arg-12, causes dramatic changes in affinity for the neuronal Na channel, the effects of charge neutralization at Arg-14, Lys-48, and Lys-49 are significantly more modest.

NMR analyses of the ApB homologs ApA, AsI (*Anemonia sulcata*), and ShI (*Stichodactyla helianthus*) (Gooley &Norton, 1986; Widmer et al., 1988; Fogh et al., 1990) are consistent with the presence of a cationic cluster formed by the side chains of Arg-14 and the C-terminal lysine, although given the flexibility in this region of the molecule in all of the solution structures, it is not possible to demonstrate the existence of such a structure conclusively. While this paper was under review, the solution structure of ApA was published (Pallaghy et al., 1995). Both this structure and models of ApB developed in our laboratory are consistent with participation of the Arg-12 guanidinium group in this cluster as well.

The model structure for ApB depicted in Figure 6 was derived from the published coordinates (pdb1sh1) for the homologous anemone toxin Sh1 (Fogh et al., 1990). Initially, the amino acid sequences of the two polypeptides were aligned so as to (1) preserve the three disulfide bonds, (2) align the conserved amino acids in loop I (Cys-6 to Leu-18; ApB numbering), and (3) align conserved amino acids in loop III (Trp-33 to Lys-48). Subsequently, appropriate amino acid substitutions were made, and the residues ^{25}Tyr-Pro^{26} of ApB were inserted between Leu-23 and Gly-24 of Sh1, in order to take into account the high homology of peptide units around these residues: Val-Asp-Leu/Leu-Trp-Phe and Gly-Ser-Cys/Ser-Cys-Gly of loop II in ShI and ApB, respectively. This insertion point is also reasonable because the Leu-Gly sequence in ShI forms an internal β-turn in loop

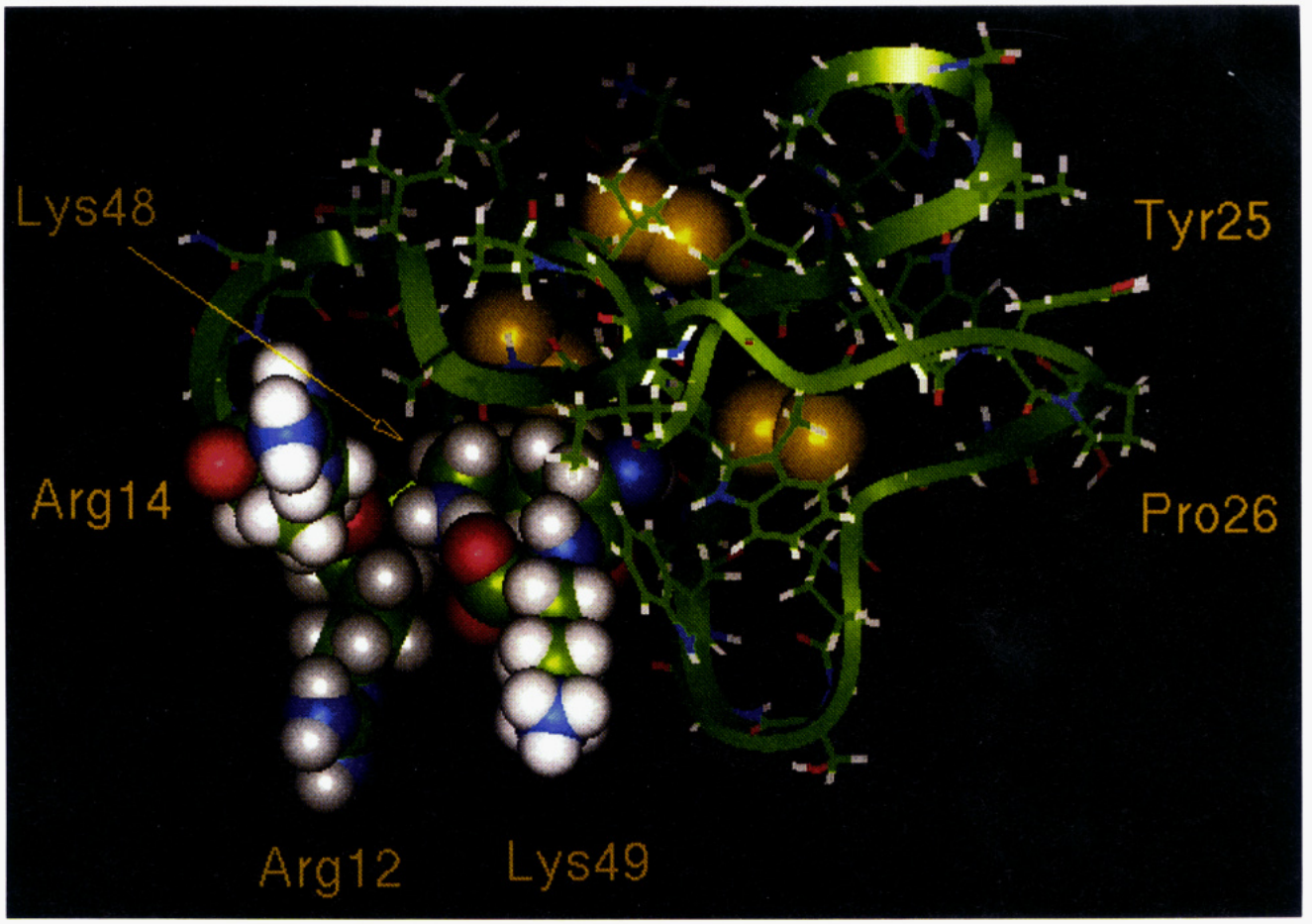

FIGURE 6: Proposed structure of ApB, modeled on the basis of the known structure of *S. helianthus* neurotoxin I (Fogh et al., 1990). The toxin backbone is shown as a ribbon, and the side chains of Arg-12, Arg-14, Lys-48, and Lys-49 are presented as space-filling models. The three disulfide bonds are indicated as large double spheres. Amino acid alignments and numbering for ShI and ApB are given below, with

```
          1         10         20         28         38
ShI    AACKCDDEG PDIRTAPLTG TVDL--GSCN AGWEKCASYY TIIADCCRKKK
ApB  GVPCLC.SD. .RP.GNT.S. ILWFYPSGCP S..HNCKAHG PNIGWCCKK--
          1         11         21         31         41
```

the cysteines indicated in bold, identical amino acids noted with dots, and missing amino acids as dashes. The β-structure content predicted from this model is 57%, consistent with the measured CD spectra. Details regarding the origin of this model are given in the text.

II with angles of rotation around backbone bonds characteristic of a type V β-turn. However, because of the conformational restrictions inherent to proline residues it proved impossible to retain all peptide bonds in the trans configuration while preserving backbone constraints for residues preceding Leu-23 and following Gly-24 in ShI. Tyr-Pro sequences have a high probability of adopting a cis configuration for the interresidue peptide bond (Fogh et al., 1990), forming a sharp type VI β-turn, and this configuration readily fit into the molecule. The recently described ApA structure includes a trans bond at this position but also indicates that cis−trans isomerization at other X-Pro bonds in the molecule does not have a major effect on overall conformation. The resulting structure was then energy minimized using Insight/Discover (Biosym Technologies, Inc., San Diego) running on a SGI Indigo with Elan Graphics. We utilized the constant valence force field and minimized using a combined steepest descents/conjugate gradients protocol. Minimization was uneventful, except for the bulky side chains of Ile-43 and Tyr-25, for which additional packing was required. Noteworthy in the predicted structure is the cluster of basic residues, including Arg-12, Arg-14, Lys-48, and Lys-49. Of these, the Lys-48 side chain appears to be located inside the molecule, with the ϵ-amino group perhaps forming a salt bridge with the C-terminal carboxylate. At the same time, the side chain of Lys-49 is in a more extended conformation, essentially parallelling that of Arg-12 and forming important components of the ApB binding site.

We emphasize that this is a predicted structure and that all known anemone toxin structures maintain a high degree of flexibility in this region (the so-called Arg-14 loop). However, the fact that single-site neutralization mutants of ApB retain a high degree of activity strongly suggests that in at least a subset of conformers these cationic functions may be juxtaposed. Although the coordinates of ApA are not as yet available in the Brookhaven database, a visual comparison of our model to that of Pallaghy et al. reveals that at a minimum the backbones of the two models are very similar.

We examined the binding affinities and channel isoform discrimination capabilities of double mutants of ApB in which two side chains of the cationic cluster are simultaneously replaced. We anticipated that this approach would allow us to ascertain whether, upon replacement of (e.g.) Arg-14, Arg-12 could assume a compensatory role in

expression of biological activity. We chose to evaluate the two highly conserved cationic sites in the double mutant R14Q-K48A, the two unique cationic sites of ApB in R12S-K49Q, and both the cationic residues of the Arg-14 loop in R12S-R14Q.

Our results show that the R14Q-K48A and R12S-R14Q mutations result in a significant loss of binding affinity in both the cell lines, the R12S-R14Q mutant being the least active in both cases. Removal of both cationic residues of the Arg-14 loop thus has a considerable effect on activity toward sodium channels. These results, combined with our prior characterization of the parental single-site mutants (Gallagher & Blumenthal, 1994; Khera & Blumenthal, 1994), suggest that the presence of one cationic residue in this loop region may be sufficient for the toxin to bind efficiently and, once bound, to stabilize the open conformation of the sodium channel. Since replacement of Arg-14 has only modest effects on toxin activity (Khera & Blumenthal, 1994), this "essential" residue must be Arg-12. The very small loss in toxicity seen previously for the R14Q mutant also raises the possibility that either Arg-12 or one of the two C-terminal lysines can play a compensatory role in this cationic cluster.

Although the mutant R12S-R14Q is the least active of all double mutants, it nonetheless displays a binding affinity of 0.5 μM in RT4-B cells and 1.6 μM in N1E-115 cells. While this represents a substantial loss of affinity, that the protein remains active suggests that neither positive charge *per se* is absolutely essential for binding affinity to either of the sodium channel isoforms or for stabilization of the open conformation of the cardiac sodium channel.

We also studied binding kinetics of mutant R12S-K49Q and of wild-type ApB and ApA by whole-cell patch clamp in both cell lines. Under these conditions, R12S-K49Q displayed an affinity for neuronal channels that is much closer to that of ApA than to that of wild-type ApB. This result confirms the importance of Arg-12 and Lys-49 for high-affinity binding of ApB to the neuronal channel isoform. However, two important differences in toxin behavior are apparent between voltage-clamp and $^{22}Na^+$ flux experiments. First, the affinity of all studied toxins for both channel isoforms is considerably higher in voltage-clamp conditions than in $^{22}Na^+$ flux. Because binding of toxins in the flux assay is carried out under Na^+-free conditions, and uptakes are measured for short times and in the presence of low $[Na^+]_{out}$, these affinity differences are not ascribable to depolarization of N1E-115 or RT-4 cells during the assays (Catterall, 1976, 1977). These differences range from a factor of 3 (ApA/neuronal) to a factor of 100 (ApB/cardiac) and in all cases are statistically significant. Second, previously reported flux assays had indicated that only ApA discriminated well between cardiac and neuronal channels. In contrast, our voltage-clamp experiments clearly demonstrate that ApB, as well as ApA and R12S-K49Q, strongly discriminates in favor of the cardiac channel over the neuronal isoform. Furthermore, these heightened preferences are not significantly different between the three toxins. (The cardiac channel is preferred by factors of 57 $\pm$ 18, 46 $\pm$ 19, and 112 $\pm$ 37, respectively.) These uniformly high selectivities contrast the relatively equal affinity of ApB for cardiac and neuronal channels in $^{22}Na^+$ flux experiments.

The physical basis underlying these differences is presently a matter of speculation, but one hypothesis seems particularly intriguing. During studies of veratridine-augmented $^{22}Na^+$ flux, the channel is maintained in a persistent open conformation. By contrast, in electrophysiological studies, membranes are clamped at a potential sufficient to ensure virtually complete maintenance of channels in the closed form. The differences in affinity may therefore arise from different binding kinetics of the toxins to the open and closed conformations of the channel. In particular, affinities for these toxins may be inherently higher for the closed state than for the open, and the ability of ApB to differentiate between channel isoforms may be heightened in the closed conformation. While it is possible that the lower apparent affinities obtained by analysis of ion fluxes reflect a direct effect of veratridine on ApB binding, we tend to disfavor this explanation. This is largely based on previous studies demonstrating that occupancy of Na channel site 2 by alkaloids enhances, rather than diminishes, the affinity of polypeptides for site 3 (Catterall, 1975; Ray et al., 1978).

It is generally recognized that the inactivated conformation of the channel has a low affinity for toxin. Early studies showed a strong voltage dependence of the site 3 scorpion toxins (Catterall, 1979; Mozahayeva et al., 1980; Stritchartz & Wang, 1986) as well as other anemone toxins (Warashina & Fujita, 1983; Warashina et al., 1988). Generally, investigators have assumed either that closed and open configurations share a similar high affinity (Gonoi et al., 1984) or that the open state has the highest affinity for toxin, although data to directly estimate differences in closed and open state affinity have been rare (Mozahayeva et al., 1980). By both methods, however, the ApB mutant R12S-K49Q combines the high binding affinity of ApB with a high selectivity for the cardiac channel isoform. These two characteristics confer upon this polypeptide features essential for the future application of the toxin in the design of new cardiotonic drugs.

REFERENCES

Barhanin, J., Hugues, M., Schweitz, H., Vincent, J.-P., & Lazdunski, M. (1981) *J. Biol. Chem. 256*, 5764−5769.

Catterall, W. A. (1975) *Proc. Natl. Acad. Sci. U.S.A. 72*, 1782−1786.

Catterall, W. A. (1976) *J. Biol. Chem. 251*, 5528−5536.

Catterall, W. A. (1977) *J. Biol. Chem. 252*, 8660−8668.

Catterall, W. A. (1979) *J. Gen. Physiol. 74*, 375−391.

Catterall, W. A. (1984) *Science 223*, 653−661.

Cleland, W. W. (1979) *Methods Enzymol. 63*, 103−138.

Donahue, L. M., Schaller, K., & Sueoka, N. (1991) *Dev. Biol. 147*, 415−424.

El Ayeb, M., Darbon, H., Bahraoui, E. M., Vargas, O., & Rochat, H. (1986) *Eur. J. Biochem. 155*, 289−294.

Fogh, R. H., Kem, W. R., & Norton, R. S. (1990) *J. Biol. Chem. 265*, 13016−13028.

Gallagher, M. J., & Blumenthal, K. M. (1992) *J. Biol. Chem. 267*, 13958−13963.

Gallagher, M. J., & Blumenthal, K. M. (1994) *J. Biol. Chem. 269*, 254−259.

Gonoi, T., Hille, B., & Catterall, W. A. (1984) *J. Neurosci. 4*, 2836−2842.

Gooley, P. R., & Norton, R. S. (1986) *Biochemistry 25*, 2349−2356.

Gould, A. R., Mabbutt, B. C., & Norton, R. S. (1990) *Eur. J. Biochem. 189*, 145−153.

Gross, G. J., Warltier, D. C., Hardman, H. F., & Shibata, S. (1985) *Eur. J. Pharmacol. 110*, 271−276.

Kem, W. R., Parten, B., Pennington, M. W., Price, D., & Dunn, B. M. (1989) *Biochemistry 28*, 3483−3489.

Kharrat, R., Darbon, H., Rochat, H., & Granier, C. (1989) *Eur. J. Biochem. 181*, 381−390.
Khera, P. K., & Blumenthal, K. M. (1994) *J. Biol. Chem. 269*, 921−925.
Kolkenbrock, H. J., Alsen, C., Asmus, R., Beress, L., & Tschesche, H. (1983) in *Proceedings of the 5th European Symposium on Animal, Plant and Microbiol. Toxins* (Mebs, D., & Habermehl, G., Eds.) p 72.
Mahnir, V. M., Kozlovskaya, E. P., & Elyakov, G. B. (1989) *Toxicon 27*, 1075−1084.
Mozahayeva, G. N., Naumov, A. P., Nosyreva, E. D., & Grishin, E. V. (1980) *Biochim. Biophys. Acta 597*, 587−602.
Newcomb, R., Yasunobu, K. T., Seriguchi, D., & Norton, T. R. in (1980) *Frontiers in Protein Chemistry* (Liu, D. T., Mamiya, G., & Yasunobu, K. T., Eds.) pp 539−550, Elsevier North-Holland, New York.
Norton, R. S. (1991) *Toxicon 29*, 1051−1084.
Pallaghy, P. K., Scanlon, M. J., Monks, S. A., & Norton, R. S. (1995) *Biochemistry 34*, 3782−3794.
Platou, E. S., Refsum, H., & Hotvedt, R. (1986) *J. Cardiovasc. Pharmacol. 8*, 459−465.
Ray, R., Morrow, C. S., & Catterall, W. A. (1978) *J. Biol. Chem. 253*, 7307−7313.
Sanger, F., Coulson, A. R., Barrell, B. G., Smith, A. J. H., & Roe, B. A. (1980) *J. Mol. Biol. 143*, 161−178.
Schweitz, H., Vincent, J.-P., Barhanin, J., Frelin, C., Linden, G., Hugues, M., & Lazdunski, M. (1981) *Biochemistry 20*, 5245−5252.
Scriabine, A., Van Arman, C. G., Morgan, G., Morris, A. A., Bennet, C. D., & Bohidar, N. R. (1979) *J. Cardiovasc. Pharmacol. 1*, 571−583.
Shibata, S., Norton, T. R., Izumi, T., Matsuo, T., & Katsuki, S. (1976) *J. Pharmacol. Exp. Ther. 199*, 298−309.
Stewart, D. E., Sarkar, A., & Wampler, J. E. (1990) *J. Mol. Biol. 214*, 253−260.
Strichartz, G. R., & Wang, G. K. (1986) *J. Gen. Physiol. 88*, 413−435.
Tamkun, M. M., & Catterall, W. A. (1981) *Mol. Pharmacol. 19*, 78−86.
Warashina, A., & Fujita, S. (1983) *J. Gen. Physiol. 81*, 305−323.
Warashina, A., Ogura, T., & Fujita, S. (1988) *Comp. Biochem. Physiol. 90C*, 351−358.
Wasserstrom, J. A., Kelly, J. E., & Liberty, K. N. (1993) *Pflugers Arch. 424*, 15−24.
Widmer, H., Wagner, G., Schweitz, H., Lazdunski, M., & Wüthrich, K. (1988) *Eur. J. Biochem. 171*, 177−192.
Zeng, D., Hanck, D. A., & Fozzard, H. A. (1993) *Soc. Neurosci. Abstr. 19* (Part 1, Abstract 121.9), 284.

BI9504320